

# Antibacterial, Antioxidant, and Raw 264.7 Cell Line Proliferative Effect of 5-[(4-Nitro-Benzylidene)-Amino]-2H-Pyrazol-3-ol

Okoli Bamidele Joseph<sup>1</sup>, Terblanche Unisa<sup>2</sup>, Ssemakalu Cornelius Cano<sup>2</sup>, Pillay Michael<sup>2</sup>, Modise Johannes Sekomeng<sup>1</sup>

<sup>1</sup>Institute of Chemical and Biotechnology, <sup>2</sup>Department of Biotechnology, Faculty of Applied and Computer Sciences, Vaal University of Technology, South Africa

## Abstract

**Introduction:** Pyrazole derivatives are considered important scaffolds that possess cocktails of pharmacological activities. However, no study has assessed their effects on the proliferation of macrophages. **Aim:** In this study, 4-nitrophenyl derivative (HL<sub>1</sub>) containing the 1*H*-pyrazol-5-ol moiety was synthesized, characterized, and assessed for antibacterial as well as cell proliferative effects. **Materials and Methods:** HL<sub>1</sub> was characterized using an elemental analyzer, thermogravimetric analysis, X-ray diffraction, and various spectrophotometric methods. The antibacterial effect of HL<sub>1</sub> on three Gram-positive bacterial strains, namely *Enterococcus faecalis*, *Staphylococcus aureus*, and *Staphylococcus epidermidis*, and three Gram-negative bacterial strains, namely *Klebsiella pneumoniae*, *Escherichia coli*, and *Pseudomonas aeruginosa*, was determined using the minimal inhibition assays. The RAW 267.4 macrophage cell line was used to assess the effect of HL<sub>1</sub> on mitochondrial activity using the CellTiter® blue cell viability assay. **Results:** The thermogram and diffractogram plots registered thermal stability slightly above the melting point of HL<sub>1</sub> and a crystal size of 13.01 nm, respectively. The characterization studies indicated the presence of azomethine moiety at 1701.65 cm<sup>-1</sup>, δ<sub>H</sub> 9.13, and δ<sub>C</sub> 156.85 ppm on the Fourier-transform infrared, <sup>1</sup>H, and <sup>13</sup>C nuclear magnetic resonance, respectively. The synthesized pyrazole moiety exhibited significant antioxidant activity (IC<sub>50</sub> ≤ 0.41 ± 0.02 μM) compared to the acid controls (IC<sub>50</sub> ≤ 0.58 ± 0.01 μM) and preserved pharmacological integrity at high temperature but was found not to have any antibacterial effects. **Conclusion:** The effect of HL1 on the Raw 267.4 cell line intimated a significant increase in the mitochondrial function of the macrophage cells (12.5 μg/ml [127 ± 3 %; P < 0.0007] vs. control) indicating an increase in cell proliferation.

**Key words:** Azomethine, diffractogram, macrophage, proliferation, radical, thermogram

## INTRODUCTION

The azole, specifically the five-membered 1*H*-pyrazol-5-ol-scaffold, has attracted attention due to the pharmacological potency acquired when coupled to an aromatic aldehyde unit.<sup>[1]</sup> The presence of the pyrazole nucleus can be traced in many pharmaceutically established drugs with diverse therapeutic activities.<sup>[2,3]</sup> Over the past two decades, pyrazole-Schiff base derivatives have found diverse applications due to their potent antioxidant, antimicrobial, antimycobacterial, anti-inflammatory, non-enzymatic protein glycation inhibition, gastric secretion stimulation, and antidepressant properties.<sup>[4-6]</sup> Many Schiff bases derived from pyrazole have been synthesized

by the condensation of 1*H*-pyrazol-3-amine derivatives and different aromatic aldehydes or ketones leading to polysubstituted pyrazole as reported by Baluja and Chanda.<sup>[7]</sup>

The continuous search for novel biologically active pyrazole derivatives coupled with the development of drug resistance

### Address for correspondence:

Dr. Okoli Bamidele Joseph, Institute of Chemical and Biotechnology, Faculty of Applied and Computer Sciences, Vaal University of Technology, South Africa.  
E-mail: okolibj@binghamuni.edu.ng

**Received:** 11-07-2018

**Revised:** 12-11-2018

**Accepted:** 22-11-2018

of microbial strains has made it necessary to investigate the influence of these compounds on biological systems. Despite the research done to develop pharmaceutically potent pyrazole derivatives, no study has targeted the effect of pyrazole on the macrophages, an essential component of the mammalian immune system. Macrophages are widely distributed throughout the different tissues where they play a role in the phagocytosis of virally infected and cancerous cells as well as extrinsic threats such as pathogen invasion or breach in tissue.<sup>[8]</sup>

In this study, we investigated the antimicrobial, antioxidant, and RAW 246.7 macrophage proliferative effects of 4-nitrophenyl derivative containing the 2*H*-pyrazol-3-ol.

## Experimental details

### Chemicals

All chemicals and reagents used in this study were of analytical grade; 3-amino-5-hydroxypyrazole, 4-nitrobenzaldehyde, 2,2-diphenyl-1-picrylhydrazyl (DPPH), quercetin, gallic acid, ascorbic acid, penicillin G, streptomycin, dimethyl sulfoxide (DMSO), hydrogen peroxide, 2,2'-azino-bis-3-ethylbenzothiazoline-6-sulfonic acid (ABTS), and potassium persulfate from Sigma-Aldrich (St. Louis, MO). Potassium ferricyanide, trichloroacetic acid, and ferric chloride were purchased from Merck (Darmstadt, Germany). Dulbecco's Modified Eagle Medium (DMEM) and fetal bovine serum (FBS) were obtained from Thermo Fisher Scientific (Waltham, MA). Others such as phosphate buffer, ethanol, and glacial acetic acid were purchased from Promark and Rochelle Chemicals (Johannesburg, South Africa), respectively.

### Instrumentation

The percentage elemental composition of the 3-(*E*)-((4-nitrophenyl) methylidene) amino)-1*H*-pyrazol-5-ol was measured using aLECO analyzer (CHNS628 analyser, Lakeview, MI). The maximum absorption, as well as the melting point, was measured using a UV-visible spectrophotometer (Agilent Technologies Cary 60, Santa Clara, CA) and Stuart digital apparatus (Vernon Hills, IL), respectively. <sup>1</sup>H- and nuclear magnetic resonance (<sup>13</sup>C-NMR) chemical shifts (ppm) were recorded using a 400 MHz NMR spectrometer (Agilent Technologies). Thermal response was monitored on a PerkinElmer, Thermogravimetric Analyzer (Perkin Elmer, Waltham, MA) operated at a temperature ranging between 30 and 900°C at a heating rate of 10°C/

min under a nitrogen atmosphere. The X-ray diffractogram (XRD) was recorded on a ZEISS Sigma 300 diffractometer (Zeiss, Oberkochen, Germany). The Spectrum 400 Fourier-transform infrared (FT-IR) (PerkinElmer) scanning between 4000 and 400 cm<sup>-1</sup> was used to determine the functional groups.

### Synthesis of 5-[(4-Nitro-Benzylidene)-Amino]-2*H*-Pyrazol-3-ol

An ethanolic solution of 3-amino-5-hydroxypyrazole (0.99 g; 9.98 mmol) was mixed with 4-nitrobenzaldehyde (3.02 g; 19.98 mmol) in 95% of ethanol. To the mixture, 0.5 mL of glacial acetic acid was introduced and refluxed for 8 h. The product (HL<sub>1</sub>) obtained was filtered, washed several times 95% ethanol, recrystallized from cold ethanol solution, and dried in an oven at 40°C. The chemical formulation of the structure of HL<sub>1</sub> is shown in Figure 1.

### Electronic absorption study

The wavelength maximum of HL<sub>1</sub> was determined at room temperature, and the molar absorptivity coefficient was calculated from the Lambert–Beer equation 1:

$$A = \epsilon_{\lambda_{\max}} bC \quad (1)$$

Where A is the absorbance, b is the path length, C is the concentration of HL<sub>1</sub> (mol/L), and  $\epsilon_{\lambda_{\max}}$  is the molar absorption coefficient (Lmol<sup>-1</sup> cm<sup>-1</sup>).

### XRD study

The XRD was investigated at 40 kV and 40 mA with Cu-K $\alpha$  ( $\lambda = 1.5406 \text{ \AA}$ ) radiation, and the crystallite size (D) was calculated using Scherrer equation (2).

$$D = K\lambda/\beta \cos\theta \quad (2)$$

Where K is the equipment constant (0.94),  $\lambda$  is the wavelength (1.5406  $\text{\AA}$ ), and  $\beta$  is the integral height to width of the diffraction peak.

### Antioxidant Assays

The antioxidant activity of HL<sub>1</sub> was evaluated and compared with three positive controls; quercetin, gallic acid, and ascorbic acid.

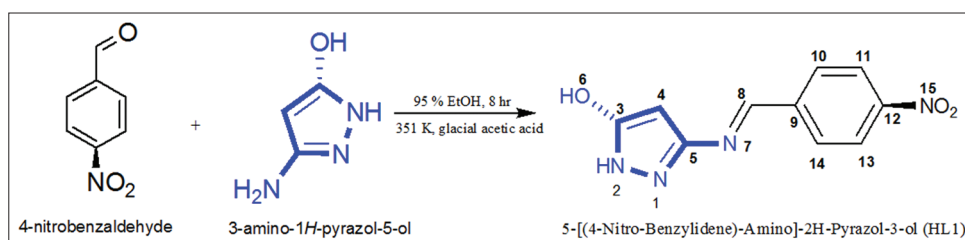


**Figure 1:** Chemical synthesis of 5-[(4-Nitro-Benzylidene)-Amino]-2*H*-Pyrazol-3-ol

**DPPH radical scavenging activity (RSA)**

The DPPH (300  $\mu\text{L}$ , 0.05 mM) radical ethanolic solution was mixed with various concentrations (4.31, 2.15, 1.08, 0.54, and 0.27  $\mu\text{M}$ ) of HL<sub>1</sub> and incubated for 30 min in the dark. Changes in the absorbance of the mixtures were measured at 517 nm on a UV-Vis spectrophotometer.<sup>[9]</sup> The percentage of RSA was calculated from equation 3 and the half maximal inhibitory concentration (IC<sub>50</sub>  $\mu\text{M}$ ) of the test compounds was determined by linear regression analysis. All analyses were carried out in triplicate.

$$\% \text{RSA} = 100 \frac{(\text{Abs. of DPPH control} - \text{Abs. of HL1})}{(\text{Abs. of DPPH control})} \quad (3)$$

**ABTS radical cation decolorization assay**

The blue-green ABTS<sup>+</sup> acid radical cation solution was prepared by dissolving 960.2 mg of ABTS in a 250 mL solution of 0.0024 mM potassium persulfate and stored away for 24 h. After that, the absorbance was adjusted to 0.9547 at 734 nm with distilled water. Exactly 40  $\mu\text{L}$  of various concentrations (4.31, 2.15, 1.08, 0.54, and 0.27  $\mu\text{M}$ ) of HL<sub>1</sub> or control was added to 3 mL of the ABTS<sup>+</sup> solution and incubated for 30 min at 25°C in the dark, and the changes in the concentration of ABTS<sup>+</sup> were measured at 734 nm. The decolorization of the blue-green solution was used as a template to evaluate the percentage proton-donating potential (%PDP) of the test compounds and estimated from equation 4.<sup>[10]</sup> The IC<sub>50</sub> ( $\mu\text{M}$ ) of the compounds was determined by linear regression analysis. All analyses were carried out in triplicate.

$$\% \text{PDP} = 100 \frac{(\text{Abs. of ABTS control} - \text{Abs. of HL1})}{(\text{Abs. of ABTS control})} \quad (4)$$

**H<sub>2</sub>O<sub>2</sub> scavenging activity**

The H<sub>2</sub>O<sub>2</sub> scavenging activity of the test compound was evaluated according to the methods of Ruch *et al.*<sup>[11]</sup> with slight modifications. To 100  $\mu\text{L}$  aliquot of the test compounds, 0.4 mL of 50 mM phosphate buffer was added followed by 0.6 mL of 2 mM H<sub>2</sub>O<sub>2</sub> solution prepared in 50 mM phosphate buffer (pH 6.8). The absorbance of the mixture was measured at 230 nm and the % H<sub>2</sub>O<sub>2</sub> scavenging activity was computed from equation 5. The IC<sub>50</sub> ( $\mu\text{M}$ ) of HL<sub>1</sub> or controls was determined by linear regression analysis. All analyses were carried out in triplicate.

$$\% \text{H}_2\text{O}_2 - \text{scavenging activity} = 100 \frac{(\text{Abs. of H}_2\text{O}_2 - \text{Abs. of HL1})}{(\text{Abs. of H}_2\text{O}_2)} \quad (5)$$

**Ferric Reducing Power**

The ferric reducing activity was determined according to the method of Oyaizu.<sup>[12]</sup> In brief, a 0.5 mL aliquot of HL<sub>1</sub> was mixed with 2 mL phosphate buffer (0.2 M, pH 6.8) and

2 mL potassium ferricyanide (0.03  $\mu\text{M}$ ) The mixture was incubated for 30 min at 45°C, followed by the addition of 2 mL of 0.61 mM trichloroacetic acid. A 2-mL portion of the above mixtures was transferred into 2 mL of distilled water and 0.4 mL ferric chloride (0.1% w/v) in a test tube. Then, the absorbance was measured at 700 nm after 10 min, and the reducing power was estimated as a function of the absorbance. The same protocol was applied to the controls, and all determinations were carried out in triplicate.

**Cell culture**

A murine macrophage cell line RAW 264.7 (Cellonex, Johannesburg, South Africa) was cultured and maintained in complete cell culture medium consisting of DMEM supplemented with 10% FBS and antibiotics (10,000 U/ml penicillin G and 10 mg/mL streptomycin) at 37°C in a 5% CO<sub>2</sub> incubator (ESCO, Horsham, PA). The culture medium was replaced with fresh medium every 3 days until the cells were 80% confluent. The cells were washed, trypsinized, and prepared for the cell proliferation assay.

**Cell proliferation assay**

The effect of HL<sub>1</sub> on the viability of the RAW 264.7 cell line was evaluated using the CellTiter® Blue Cell Viability Assay (Promega, Cat. No. G8081, Madison, WI) according to the manufacturer's instructions with a few modifications. The RAW 264.7 cells were seeded in a 96-well microtiter plate (100  $\mu\text{L}$  per well) at a concentration of  $5 \times 10^4$  cells/mL in complete cell culture medium and incubated at 37°C in a 5% humidified CO<sub>2</sub> incubator. After 24 h of incubation, the cell culture medium was replaced with fresh complete cell culture medium containing different concentrations of the HL<sub>1</sub> (6.25, 12.5, 25, 50, and 100  $\mu\text{g/mL}$ ). Four control groups were set up consisting of (i) cell culture medium only (negative control to determine background absorbance), (ii) untreated cells (vehicle control), (iii) medium with 0.1% DMSO (used as solvent for compound), and (iv) cells treated with hydrogen peroxide (H<sub>2</sub>O<sub>2</sub>) used as the negative control. After treatment, the cells were incubated for different time intervals (24, 96, and 168 h) at 37°C in a humidified 5% CO<sub>2</sub> incubator. At the end of each incubation period, 20  $\mu\text{L}$ /well of CellTiter® Blue Reagent was added to each well containing the remaining culture medium. The plate was then agitated for 10 s and incubated at 37°C for 4 h in a humidified 5% CO<sub>2</sub> incubator. Thereafter, 100  $\mu\text{L}$  medium containing CellTiter® Blue reagent was transferred into a 96-well microtiter plate, and the absorbance of the dissolved resorufin dye was determined at 570 and 600 nm, respectively, using an EPOCH 2 (BioTek, Winooski, VT) plate reader.

**Antibacterial property****Bacterial strains**

The microorganisms used in the present investigation included reference strains from the American Type Culture Collection

(ATCC) and the National Collection of Type Cultures (NCTC). These included three Gram-positive bacterial strains: *Enterococcus faecalis* (ATCC 49533), *Staphylococcus aureus* (obtained from a local hospital in Vanderbijlpark, South Africa), and *Staphylococcus epidermidis* (ATCC 12228) and three Gram-negative bacterial strains: *Klebsiella pneumoniae* (ATCC BAA-1706), *Escherichia coli* (NCTC 11954), and *Pseudomonas aeruginosa* (ATCC 25619). All the bacterial strains were individually inoculated in Mueller-Hinton Broth and incubated for 24 h before use in the broth microdilution method.

### Antibacterial activity

The antibacterial activity of the synthesized compound (HL<sub>1</sub>) was evaluated against the selected bacterial strains using the broth microdilution method as described by de Rapper *et al.*<sup>[13]</sup> and Akhalwaya *et al.*<sup>[14]</sup> with slight modifications. A 1000 mg/mL stock solution of HL<sub>1</sub>, dissolved in DMSO, was diluted to a working concentration of 300 mg/mL. Microtiter 96-well plates (Nunc Roskilde, Denmark) were prepared by adding 100  $\mu$ L sterilized deionized water aseptically to each well. Thereafter, 100  $\mu$ L of the test compound (HL<sub>1</sub>) was added to the first row of each microtiter plate. Two-fold serial dilutions were carried out down each column to obtain concentrations from 150 to 1.17 mg/mL at a total volume of 100  $\mu$ L per well. Standardized bacterial cultures (100  $\mu$ L) at a concentration of  $1 \times 10^6$  colony-forming units/mL were then added to each well of their respective microtiter plates. To detect bacterial growth, 30  $\mu$ L resazurin indicator dye (0.015%) was added to each well before incubation. Resazurin is an oxidation-reduction indicator that undergoes colorimetric changes (from blue to pink or colorless) in response to reduction by mitochondrial reductases and other diaphorases such as dihydrolipoamide dehydrogenase, NAD(P)H: quinone oxidoreductase, and flavin reductase.<sup>[15]</sup> The inoculated microtiter plates were sealed using a sterile adhesive film and incubated at 37°C for 24 h. Amoxycillin (2.5 mg/mL) (Melford, Chelsworth, United Kingdom) and neomycin (2.5 mg/ml) were included as positive controls. DMSO was included as a negative control to confirm that the solvent did not exert any antibacterial effect and a culture control ensured that the broth could support bacterial growth. According to the

Clinical Laboratory Standards Institute guidelines for broth microdilution,<sup>[16]</sup> the Minimum inhibitory concentration (MIC) is defined as the lowest concentration that completely inhibits the microorganism from multiplying and producing visible growth in the test solution. After inspection of the microtiter plates, 10  $\mu$ L of the MIC well content was plated on nutrient agar plates and incubated for another hour at 37°C to confirm the antibacterial property of the synthesized compound. All experiments were done in triplicate.

### Statistical analysis

Statistical analysis was carried out with OriginPro software (Origin Lab Corporation, Northampton, MA 01060 USA), and the results are expressed as means  $\pm$  standard deviation.

## RESULTS

### Chemistry of

#### 5-[(4-Nitro-Benzylidene)-Amino]-2*H*-Pyrazol-3-ol

The product (HL<sub>1</sub>) was collected as a regatta powder. Yield 61.8%; m.p 283–285°C;  $\lambda_{\text{max}}$  393 nm and  $\epsilon$  [Figure 2a]; IR (cm<sup>-1</sup>) 3352 (w), 3108.16 (w), 2859.43 (w), 1701.65 (m), 1623.64 (m), 1515.20, 1344.38(s), 1198.68, 1107.27, 1013.70 (m), 856.00 and 814.24 (m), 697.03 (m) [Figure 2b]. <sup>1</sup>H NMR (400 MHz, DMSO-*d*<sub>6</sub>)  $\delta$  9.13 (s, 1H), 8.35–8.28 (m, 2H), 8.19–8.11 (m, 2H), 6.34 (s, 1H), 4.01(s, 1H), 2.53(s, 1H) [Figure 3]. <sup>13</sup>C NMR (100 MHz, DMSO-*d*<sub>6</sub>)  $\delta$  160.47, 156.85, 152.56, 149.35, 139.05, 129.41, 129.43, 124.39, 124.40, 85.93 [Figures 4]. Anal. calculated for C<sub>10</sub>H<sub>8</sub>N<sub>4</sub>O<sub>3</sub>: %C, 51.73; %H, 3.47; %N, 24.13. Found: %C 51.17, %H 3.97, %N 24.76.

### Thermal profile of

#### 5-[(4-Nitro-Benzylidene)-Amino]-2*H*-Pyrazol-3-ol

The thermogravimetric plot of HL<sub>1</sub> is presented in Figure 5. Four major exothermic peaks corresponding to

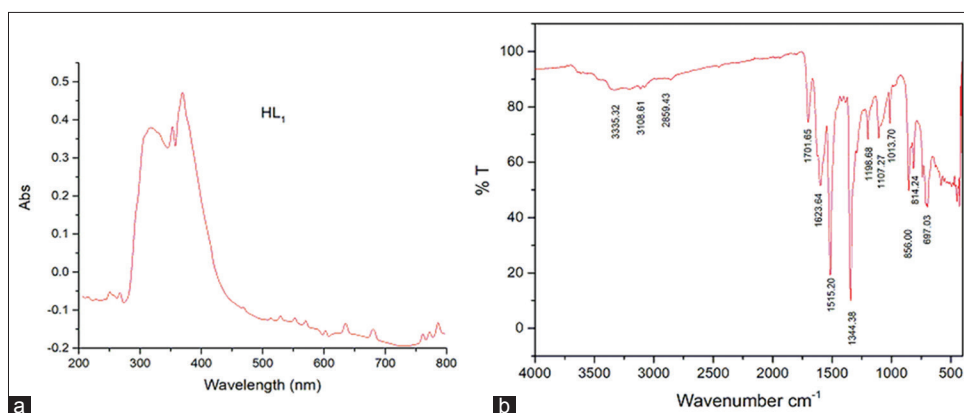


**Figure 2:** (a) UV-visible spectrum and (b) Functional group spectrum of 5-[(4-Nitro-Benzylidene)-Amino]-2*H*-Pyrazol-3-ol (HL<sub>1</sub>)

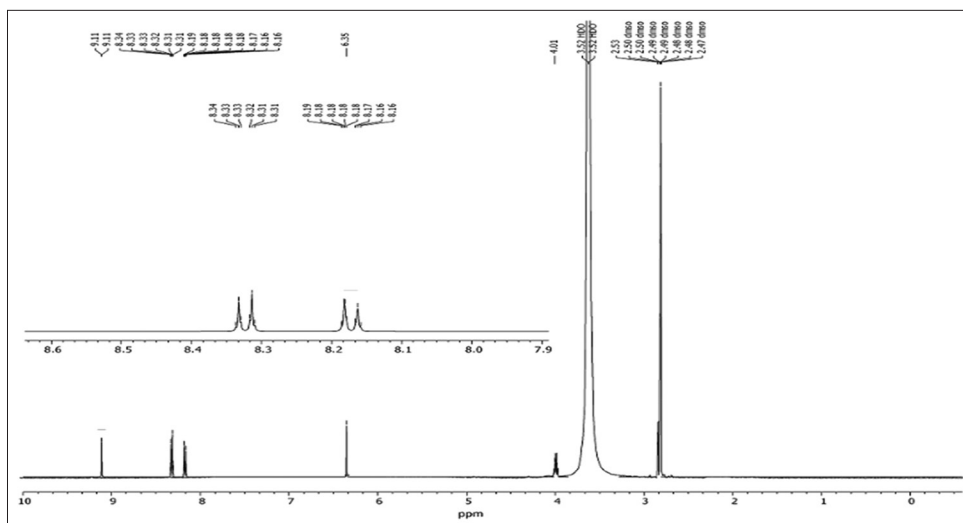
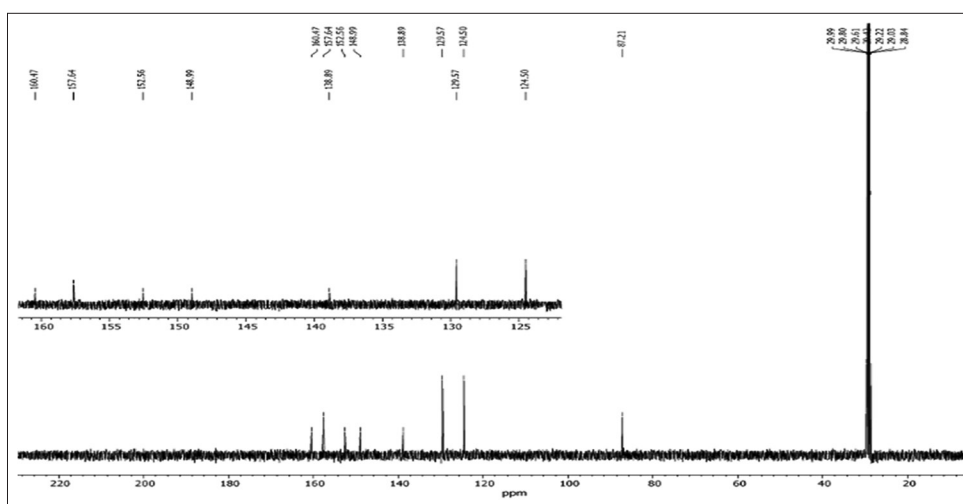


Figure 3: <sup>1</sup>H NMR spectrum of 5-[(4-Nitro-Benzylidene)-Amino]-2*H*-Pyrazol-3-ol



The diffractogram registered seven (7) reflection peaks in the range of 0–70° with a maximum at 34.24° and the crystal size determined using Scherrer formula (Eq2) was 13.01 nm.

### Antioxidant activity of 5-[(4-Nitro-Benzylidene)-Amino]-2*H*-Pyrazol-3-ol

The antioxidant activities of HL<sub>1</sub> and controls were evaluated using *in vitro* assays such as DPPH, ABTS, H<sub>2</sub>O<sub>2</sub> scavenging, and ferric reducing power. The IC<sub>50</sub> values for the different assays were obtained from the plots of the % radical inhibition against concentration with  $r^2 \geq 0.9635$  [Table 1].

The IC<sub>50</sub> values of HL<sub>1</sub> were significant ( $P < 0.05$ ) compared to the controls. HL<sub>1</sub> showed very potent radical scavenging potential with IC<sub>50</sub> of  $0.29 \pm 0.09$ – $0.41 \pm 0.02$   $\mu$ M [Table 1] and ferric reducing power of  $0.0045 \pm 0.07$  [Figure 7] compared to gallic acid and ascorbic acid, with quercetin being slightly more potent.

### Effect of HL<sub>1</sub> on cell viability

When the raw 264.7 cells were stimulated for a day with HL<sub>1</sub> at concentrations of 6.5, 12.5, 25, and 50  $\mu$ g/ml, an increase in cell viability was observed [Figure 5]. HL<sub>1</sub> at a concentration of 12.5  $\mu$ g/ml resulted in a highly significant ( $P < 0.0007$ ) increase in cell viability ( $127 \pm 3\%$ ) compared to the untreated cells ( $100 \pm 3\%$ ). When HL<sub>1</sub> was used at 100  $\mu$ g/ml, a significant

( $P < 0.009$ ) reduction in cell viability ( $83 \pm 1\%$ ) in comparison to the untreated cells was observed after day 1. When the RAW 264.7 cells were stimulated with HL<sub>1</sub> at 6.5, 12.5, 25, and 50  $\mu$ g/ml for 4 days, a slight but non-significant increase in cell viability was observed. However, 4 days of stimulation of the RAW 264.7 cells with HL<sub>1</sub> at a concentration of 100  $\mu$ g/ml resulted in a further significant ( $P < 0.001$ ) decrease in cell viability ( $47 \pm 4.68\%$ ) compared to the untreated cells ( $100 \pm 1.84\%$ ). After 7 days of stimulation with HL<sub>1</sub> at concentrations of 12.5, 25, and 50  $\mu$ g/ml, percentage cell viability remained slightly higher than that observed in the untreated cells. However, the percentage viability ( $107 \pm 0.96\%$ ) in cells stimulated with HL<sub>1</sub> at a concentration of 12.5  $\mu$ g/ml was highly significant ( $P < 0.00008$ ) than that observed in the untreated cells ( $100 \pm 3.04\%$ ). On the contrary, 7 days of stimulation with HL<sub>1</sub> at a concentration of 6.5  $\mu$ g/ml resulted in a highly significant ( $P < 0.0009$ ) decrease in cell viability ( $76 \pm 1.96\%$ ) compared to that observed in the untreated cells ( $100 \pm 3.04\%$ ). A highly significant ( $P < 0.0004$ ) decrease in the percentage cell viability ( $40 \pm 4.56\%$ ) was observed when HL<sub>1</sub> was used at a concentration of 100  $\mu$ g/ml in comparison to the untreated cells.

### Antibacterial activity

The results of the antibacterial activity of 5-[(4-Nitro-Benzylidene)-Amino]-2*H*-Pyrazol-3-ol (HL<sub>1</sub>) against the six bacterial strains using the broth microdilution method are summarized in Table 2. Amoxicillin and neomycin (2.5 mg/ml) were used as reference antibiotics for comparison purposes. The results showed predominately similar antibacterial activity against the selected bacterial strains [Table 2].

## DISCUSSION

### Spectroscopic data of 5-[(4-Nitro-Benzylidene)-Amino]-2*H*-Pyrazol-3-ol (HL<sub>1</sub>)

Two bands were observed on the electronic absorption spectrum of 0.02  $\mu$ M, 5-[(4-Nitro-Benzylidene)-Amino]-2*H*-Pyrazol-3-ol included as supplementary materials [Figures 2a]. The two bands with wavelengths of 316 and 393 nm are typical of  $n-\pi^*$  transitions and the  $\pi-\pi^*$  transitions of the aromatic rings and azomethine group, respectively.<sup>[17]</sup> The <sup>1</sup>H and <sup>13</sup>C NMR

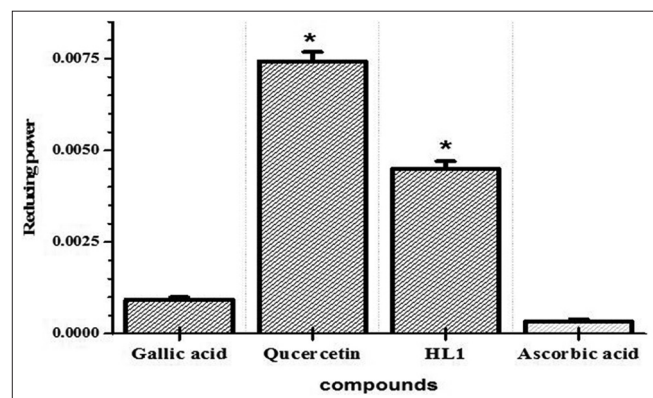


**Figure 7:** Total reducing power of 5-[(4-Nitro-Benzylidene)-Amino]-2*H*-Pyrazol-3-ol and controls (0.2 mg/mL) measured at 700 nm. The values are expressed as means  $\pm$  SD ( $n = 3$ ). \*Significant parameters;  $P < 0.05$

**Table 1:** Scavenging activity of 5-[(4-Nitro-Benzylidene)-Amino]-2*H*-Pyrazol-3-ol

Compounds	DPPH assay		ABTS assay		H <sub>2</sub> O <sub>2</sub> scavenging activity	
	IC <sub>50</sub> ( $\mu$ M)	$R^2$	IC <sub>50</sub> ( $\mu$ M)	$R^2$	IC <sub>50</sub> ( $\mu$ M)	$R^2$
HL <sub>1</sub>	$0.29 \pm 0.09$	0.9943	$0.41 \pm 0.02$	0.9953	$0.35 \pm 0.26$	0.9635
Quercetin	$0.24 \pm 0.03$	0.9891	$0.27 \pm 0.01^*$	0.9849	$0.27 \pm 2.11^*$	0.9857
Gallic acid	$0.42 \pm 0.09^*$	0.9917	$0.58 \pm 0.01$	0.9959	$0.46 \pm 0.22$	0.9728
Ascorbic acid	$0.35 \pm 0.07$	0.9965	$0.53 \pm 0.02$	0.9947	$0.44 \pm 1.51$	0.9740

The values are expressed as means  $\pm$  SD ( $n = 3$ ). \*Significant parameters;  $P < 0.05$

**Table 2:** The *in vitro* antibacterial activity of HL<sub>1</sub> using the broth microdilution method

Bacterial strains	Minimum inhibitory concentration in mg/ml			
	HL1 compound	DMSO	Antibacterial agents	
			Amoxicillin	Neomycin
Gram-positive				
<i>Enterococcus faecalis</i>	9.38*	-	0.31	1.25
<i>Staphylococcus aureus</i>	4.69*	-	<0.005	<0.005
<i>Staphylococcus epidermidis</i>	4.69*	-	<0.005	<0.005
Gram-negative				
<i>Klebsiella pneumonia</i>	9.38*	-	0.31	<0.005
<i>Escherichia coli</i>	9.38*	-	<0.005	<0.005
<i>Pseudomonas aeruginosa</i>	9.38*	-	<0.005	<0.005

\*Indicates that the mean had a  $P < 0.05$  in comparison to controls

spectra of HL<sub>1</sub> confirm the presence of azomethine group with proton and carbon signals at  $\delta$  9.13 (s, 1H) and  $\delta$  156.85 ppm, respectively, and further confirmation was observed at 1701.65  $\text{cm}^{-1}$  on the FT-IR spectrum.<sup>[18]</sup> The deshielded carbon signal at  $\delta$  162.42 ppm confirms the presence of an oxymethine unit of the pyrazol-5-ol moiety. Signals from the aromatic protons were observed at 8.35–8.11 ppm while the corresponding aromatic carbons, peaked at  $\delta$  152.56(C-5), 149.35 (C-12), 139.05(C-9), 129.57 (C-14), 129.57 (C-10) 124.50 (C-11), 124.50 (C-13), and 87.21(C-4) ppm [Figures 4]. The sharp absorption bands in the fingerprint region at 1575–1507  $\text{cm}^{-1}$  is in concordance with the aromatic signals on the <sup>1</sup>H and <sup>13</sup>C NMR spectra.<sup>[19]</sup> Other notable characteristic bands at 1623.64 and 1515.20  $\text{cm}^{-1}$  are attributed to the bending and stretching vibrations of –N–H and –O–N, with the corresponding proton signals at 2.53 (H-2) and 4.01(H-6) ppm, respectively.

### Thermal profile of 5-[(4-Nitro-Benzylidene)-Amino]-2*H*-Pyrazol-3-ol (HL<sub>1</sub>)

The thermal profile of HL<sub>1</sub> at the operating temperature of 30–900°C and the mechanism of thermal decomposition are presented in Figures 5 and 8, respectively. The thermogravimetric analysis and DTA plots revealed four thermal events at 80°C, 100°C, 287°C, and 430°C with a corresponding weight loss of 3%, 9%, 20%, and 48%, respectively. The mass loss of 3% at 80°C and 9% at 100°C is attributed to the removal of crystallizing solvent (ethanol) and adsorbed moisture, respectively. The presence of adsorbed moisture is an indication of the hygroscopic nature of HL<sub>1</sub>.<sup>[20]</sup> After dehydration, above the melting point (283°C), the first thermal decomposition step took place at 287°C, corresponding to the lost nitrogen (IV) oxide which accounts for 20% of the weight of HL<sub>1</sub> to produce 3-(*E*)-((phenylmethylidene)amino)-1*H*-pyrazol-5-ol (III). At a temperature >430°C, the compound (III) carbonizes corresponding to 48% weight loss [Figure 6]. The evaluation of the thermal profile proved that 3-(*E*)-(((4-nitrophenyl)methylidene) amino)-1*H*-pyrazol-5-ol is slightly stable above the melting point. Thereafter, the integrity of the compound

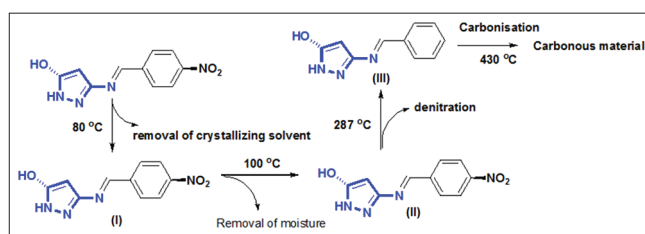


**Figure 8:** Mechanism of thermal decomposition of 5-[(4-Nitro-Benzylidene)-Amino]-2*H*-Pyrazol-3-ol

becomes compromised due to the denitration leading to the production of 3-(*E*)-((phenylmethylidene)amino)-1*H*-pyrazol-5-ol (III).

### XRD

The X-ray powder diffraction study was conducted to study the specific chemistry, atomic arrangement, and crystallinity of HL<sub>1</sub>. The diffractogram of HL<sub>1</sub> recorded seven crystalline peaks confirming the crystallinity of HL<sub>1</sub>. The nanocrystalline size of 13.01 nm calculated from the Scherrer equation (2) is an important residual factor associated with the ordered arrangement of atoms in a crystalline, which directly influences the compound properties.<sup>[21]</sup> According to the study of Carballo and Wolf<sup>[22]</sup>, the rate of biological interaction of a compound is significantly influenced by the crystallite size. Hence, the large crystallite size is expected to have some degree of influence on the biological activity.

### Antioxidant activity of HL<sub>1</sub>

Derivatives of pyrazole have been known to exhibit significant *in vitro* antioxidant activity and *in vivo* COX-II inhibition.<sup>[23]</sup> Our investigation into the antioxidant potential of HL<sub>1</sub> showed similar scavenging potentials against DPPH, ABTS acid, and peroxide radicals [Table 1] compared to the acid controls as observed in previous studies.<sup>[24-26]</sup> The total antioxidant potential of HL<sub>1</sub> was effectively estimated by the

reduction of Fe<sup>3+</sup> to Fe<sup>2+</sup> as a function of HL<sub>1</sub> to donate either an electron to the vacant *d*-orbital or proton which invariably is measured as the reduction capacity of the evaluated compound.<sup>[27]</sup> Consequently, in this study, the reducing power is in the order of quercetin > HL<sub>1</sub> > gallic acid > ascorbic acid [Figure 7]. There is a significant difference ( $P < 0.05$ ) in the ferric reducing power, with HL<sub>1</sub> showing comparative activity to quercetin. The scavenging potentials and total reducing power can be justified by the structural features of the ring structures such as the hydroxyl, carboxylic acid, or lactone groups.<sup>[28]</sup> The number of -OH groups and the ability to delocalize electrons within the complex structure to stabilize the phenoxy and carboxylate ions<sup>[29,30]</sup> influenced the antioxidant activity of quercetin relative to HL<sub>1</sub>.

### Antibacterial activity

Infectious diseases, resulting in approximately 50,000 deaths per day, remain one of the leading health-related problems worldwide. The efficacy of many of the currently available antibacterial agents that kill or prevent the reproduction of microorganisms is rapidly declining due to the emergence of multidrug-resistant organisms. Furthermore, infections caused by multidrug-resistant bacteria are associated with prolonged treatment regimens, resulting in an increased financial burden on the health-care sector.<sup>[31]</sup> The urgent need for the development of new classes of antibacterial agents is evident. However, the synthesis of new antibacterial agents is restricted by the search for new substances that are effective against microorganisms but non-toxic to mammalian cells. The antibacterial properties of pyrazole and many pyrazole derivatives have been investigated with variable degrees of antibacterial potential.<sup>[1]</sup> In the current study, the newly synthesized lactam-type Schiff base pyrazole derivative was tested for its antibacterial activity against *E. faecalis*, *S. aureus*, *S. epidermidis*, *K. pneumoniae*, *E. coli*, and *P. aeruginosa* with amoxicillin. The investigation revealed that HL<sub>1</sub> was active against all the tested bacterial strains and that the solvent, DMSO, had no inhibitory effect on any of the tested bacterial strains [Table 2]. Based on the results, a similar MIC value (9.38 mg/ml) was recorded for *K. pneumoniae*, *E. coli*, *P. aeruginosa*, and *E. faecalis*, with a slightly lower MIC value (4.69 mg/ml) for *S. epidermidis* and *S. aureus*. Studies have indicated that Gram-negative bacteria are more resistant to antimicrobial agents as compared to Gram-positive bacteria due to the presence of a mostly impermeable cell wall.<sup>[32]</sup> On comparing the antibacterial potential of the newly synthesized Schiff base with that of the reference compounds (amoxicillin and neomycin), it was concluded that HL<sub>1</sub> displayed poor antibacterial activity against all tested bacterial strains.

### Effect of HL<sub>1</sub> on cell proliferation

The results showed that HL<sub>1</sub> at low concentrations, particularly at 12.5 µg/ml, significantly increased the number

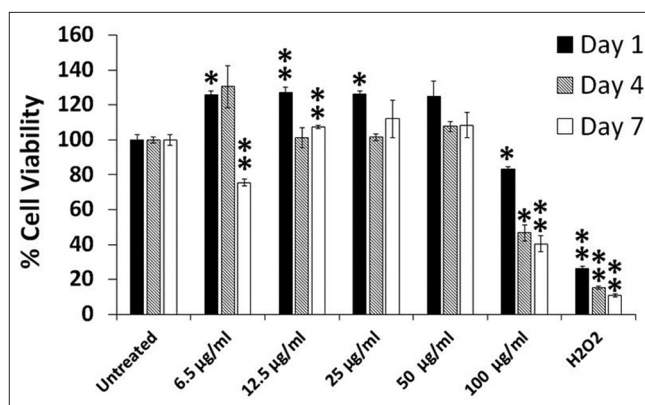


**Figure 9:** Percentage viability following the stimulation of RAW 264.7 cells with HL<sub>1</sub> at 6.5, 12.5, 25, 50, and 100 µg/ml for 1, 4, and 7 days. The untreated cells were used as a negative control, whereas the H<sub>2</sub>O<sub>2</sub> was used as a positive control. The error bars indicate the standard error of the mean of quadruplicate experiments. \*Indicates that the mean had  $P < 0.05$  in comparison to the untreated cells. \*\*Indicates that the mean had  $P < 0.0001$  in comparison to the untreated control

of viable macrophage cells [Figure 9]. The increase in cell viability is, perhaps, due to an increase in mitochondrial activity which could have resulted from the proliferation or self-renewal of the macrophages. The link between an increase in mitochondrial activity and cell proliferation has been established in various studies.<sup>[33,34]</sup> Clearly, the results showed that HL<sub>1</sub> could act as a macrophage growth factor although the exact mode of action remains unknown. It is possible that the HL<sub>1</sub> could have promoted the proliferation of macrophages through the upregulation of the colony-stimulating factor (CSF) receptors. The proliferation or self-renewal of macrophages *in vivo* has been documented and is shown to result from the presence of growth factors and cytokines such as macrophage M-CSF or granulocyte-macrophage stimulating factor GM-CSF<sup>[8]</sup> and IL-4<sup>[8,35]</sup> or IL-34.<sup>[36]</sup> Similar reasons could be forwarded for the proliferation of macrophages in this study. Furthermore, the proliferation of macrophages has been linked to the increased expression of the CSF 1 receptor.<sup>[8]</sup> Although a time-based decrease in the proliferative capability of HL<sub>1</sub> was observed, while proliferation remained above that observed in the untreated macrophages. The ability for HL<sub>1</sub> to induce a sustained increase in macrophage proliferation could either result in a positive or negative outcome. The proliferation of resident macrophages is desirable for pathogen control or wound repair, especially in a situation, where an inflammatory response could have resulted in the depletion of the resident macrophages.<sup>[35]</sup> On the contrary, macrophage proliferation has also been associated with inflammatory pathology such as in obesity-associated tissue inflammation<sup>[37]</sup> and type II diabetes.<sup>[38]</sup> However, the negative or positive outcome largely would depend on whether the resident macrophages are either classically M1 or M2 activated. The M1 macrophages are associated with the production of pro-inflammatory cytokine and phagocytosis and play a vital role in the initiation of

an immune response, whereas the M2 macrophages induce proliferation and are associated with wound healing and tissue repair.<sup>[39]</sup> The potential applications that might involve HL<sub>1</sub> should take into cognizance the ability of this compound to induce and maintain macrophage proliferation.

## CONCLUSION

Our study underlines the fact that this pyrazole derivative (HL<sub>1</sub>) is stable beyond the melting point with potent antioxidant potentials but poor antibacterial activity. Future work will focus on profiling the cytokines and chemokines produced by the macrophages in response to HL<sub>1</sub>. Furthermore, gene and protein expression studies will be done to establish the influence that HL<sub>1</sub> may have on the expression of CSF-1R. This will provide some information on the mechanism through which HL<sub>1</sub> was able to induce and sustain macrophage proliferation. This approach could provide a basis for the practical applications of HL<sub>1</sub>.

## REFERENCES

- Karrouchi K, Radi S, Ramli Y, Taoufik J, Mabkhot YN, Al-Aizari FA, *et al.* Synthesis and pharmacological activities of pyrazole derivatives: A review. *Molecules* 2018; 23:23010134.
- Khan MF, Alam MM, Verma G, Akhtar W, Akhter M, Shaquiquzzaman M, *et al.* The therapeutic voyage of pyrazole and its analogs: A review. *Eur J Med Chem* 2016; 120:170-201.
- Kumar AK, Jayaroopa P. Pyrazoles: Synthetic strategies and their pharmaceutical applications - An overview. *Int J PharmTech Res* 2013;5:1473-86.
- Kameyama T, Nabeshima T. Effects of 1,3-diphenyl-5-(2-dimethylaminopropionamide)-pyrazole[difenamizole] on a conditioned avoidance response. *Neuropharmacology* 1978;17:249-56.
- Luttinger D, Hlasta DJ. Antidepressant agents. *Ann Rep Med Chem* 1987;22:21-30.
- Hampp C, Hartzema A. P03 cost-utility analysis of rimonabant in the treatment of obesity. *Value Health* 2006;9:90.
- Baluja S, Chanda S. Synthesis, characterization and antibacterial screening of some Schiff bases derived from pyrazole and 4-amino antipyrine. *Rev Colomb Cienc Químico Farm* 2016;45:201.
- Italiani P, Boraschi D. From monocytes to M1 M2 macrophages: Phenotypical vs. Functional differentiation. *Front Immunol* 2014;5:514.
- Blois MS. Antioxidant determinations by the use of a stable free radical. *Nat* 1958;181:1199-200.
- Wolfenden BS, Willson RL. Radical-cations as reference chromogens in kinetic studies of one-electron transfer reactions: Pulse radiolysis studies of 2,2'-azinobis-(3-ethylbenzthiazoline-6-sulphonate). *J Chem Soc Perkin Trans* 1982;2:805-12.
- Ruch RJ, Cheng SJ, Klaunig JE. Prevention of cytotoxicity and inhibition of intercellular communication by antioxidant catechins isolated from chinese green tea. *Carcinogenesis* 1989;10:1003-8.
- Oyaizu M. Antioxidative activities of browning products of glucosamine fractionated by organic solvent and thin layer chromatography. *Nippon Shokuhin Kogyo Gakkaishi* 1988;35:771-5.
- de Rapper S, Kamatou G, Viljoen A, van Vuuren S. The *in vitro* antimicrobial activity of lavender angustifolia essential oil in combination with other aromatic therapeutic oils. *Evid Based Complement Alternat Med* 2013;2013:852049.
- Akhalwaya S, van Vuuren S, Patel M. An *in vitro* investigation of indigenous south african medicinal plants used to treat oral infections. *J Ethnopharmacol* 2018;210:359-71.
- Rampersad SN. Multiple applications of alamar blue as an indicator of metabolic function and cellular health in cell viability bioassays. *Sensors (Basel)* 2012;12:12347-60.
- Subramaniam P, Nandan N. Effect of xylitol, sodium fluoride and triclosan containing mouth rinse on *Streptococcus mutans*. *Contemp Clin Dent* 2011; 2:287-90.
- Petrus ML, Bouwer RK, Lafont U, Athanasopoulos S, Greenham NC, Dingemans TJ. Small-molecule azomethines: Organic photovoltaics via Schiff base condensation chemistry. *J Mater Chem A* 2014;2:9474-7.
- Wawer V, Koleva T, Dudev I. <sup>1</sup>H and <sup>13</sup>C NMR study and AM1 calculations of some azobenzenes and N-benzylideneanilines: Effect of substituents on the molecular planarity. *J Mol Struct* 1997;412:153-9.
- Malladi S, Isloor AM, Isloor S, Akhila DS, Fun HK. Synthesis, characterization and antibacterial activity of some new pyrazole based Schiff bases. *Arab J Chem* 2013; 6:335-40.
- Soliman EA, El-Kousy SM, Abd-Elbary HM, Abou-zeid AR. Low molecular weight chitosan-based Schiff bases: Synthesis, characterization and antibacterial activity. *Am J Food Technol* 2013;8:17-30.
- Ohira T, Yamamoto O. Correlation between antibacterial activity and crystallite size on ceramics. *Chem Eng Sci* 2012; 68:355-61.
- Carballo LM. During the catalytic Pt/-Al<sub>2</sub>O<sub>3</sub>. Oxidation of propylene. *J Catal* 1978;53:366-73.
- Naim MJ, Alam O, Nawaz F, Alam MJ, Alam P. Current status of pyrazole and its biological activities. *J Pharm Bioallied Sci* 2016;8:2-17.
- Aburas NM. Faculty of Chemistry Electrochemical Behaviour and Antioxidant Activity of Tetradentate Schiff Bases and Their Copper(II) Complexes. Belgrade: University of Belgrade; 2014.
- Pasupala P. Synthesis and antioxidant studies of schiff bases of 2-pyrazole substituted quinoline derivatives. *Res J Pharm Biol Chem Sci* 2017;8:1415-20.
- Karrouchi K, Chemlal L, Taoufik J, Cherrah Y, Radi S, El

- Abbes Faouzi M, *et al.* Synthèse, activités anti-oxydantes et analgésiques de bases de Schiff dérivées du 4-amino-1,2,4-triazole porteur d'un noyau pyrazole. *Ann Pharm Fr* 2016;74:431-8.
27. Siddhuraju P, Mohan PS, Becker K. Studies on the antioxidant activity of Indian *Laburnum* (*Cassia fistula* L.): A preliminary assessment of crude extracts from stem bark, leaves, flowers and fruit pulp. *Food Chem* 2002;79:61-7.
28. Shukla S, Mehta A, Bajpai VK, Shukla S. *In vitro* antioxidant activity and total phenolic content of ethanolic leaf extract of stevia rebaudiana bert. *Food Chem Toxicol* 2009;47:2338-43.
29. Silva FA, Borges F, Ferreira MA. Effects of phenolic propyl esters on the oxidative stability of refined sunflower oil. *J Agric Food Chem* 2001;49:3936-41.
30. Joyeux M, Lobstein A, Anton R, Mortier F. Comparative antilipoperoxidant, antinecrotic and scavenging properties of terpenes and biflavones from *Ginkgo* and some flavonoids. *Planta Med* 1995;61:126-9.
31. Cole ST. Who will develop new antibacterial agents? *Philos Trans R Soc Lond B Biol Sci* 2014;369:20130430.
32. Malanovic N, Lohner K. Gram-positive bacterial cell envelopes: The impact on the activity of antimicrobial peptides. *Biochim Biophys Acta* 2016;1858:936-46.
33. Antico Arciuch VG, Elguero ME, Poderoso JJ, Carreras MC. Mitochondrial regulation of cell cycle and proliferation. *Antioxid Redox Signal* 2012;16:1150-80.
34. van den Bogert C, Spelbrink JN, Dekker HL. Relationship between culture conditions and the dependency on mitochondrial function of mammalian cell proliferation. *J Cell Physiol* 1992;152:632-8.
35. Jenkins SJ, Ruckerl D, Cook PC, Jones LH, Finkelman FD, van Rooijen N, *et al.* Local macrophage proliferation, rather than recruitment from the blood, is a signature of TH2 inflammation. *Science* 2011;332:1284-8.
36. Jenkins SJ, Ruckerl D, Thomas GD, Hewitson JP, Duncan S, Brombacher F, *et al.* IL-4 directly signals tissue-resident macrophages to proliferate beyond homeostatic levels controlled by CSF-1. *J Exp Med* 2013;210:2477-91.
37. Amano SU, Cohen JL, Vangala P, Tencerova M, Nicoloro SM, Yawe JC, *et al.* Local proliferation of macrophages contributes to obesity-associated adipose tissue inflammation. *Cell Metab* 2014;19:162-71.
38. Braune J, Weyer U, Hobusch C, Mauer J, Brüning JC, Bechmann I, *et al.* IL-6 regulates M2 polarization and local proliferation of adipose tissue macrophages in obesity. *J Immunol* 2017;198:2927-34.
39. Martinez FO, Gordon S. The M1 and M2 paradigm of macrophage activation: Time for reassessment. *F1000Prime Rep* 2014;6:13.

**Source of Support:** Nil. **Conflict of Interest:** None declared.